dendritic intracellular Ca^{2+} transients (Fig. 7). Thus, it is likely that, in humans, the psychoactive effects caused by MAM-2201 are mainly due to inhibition of neurotransmitter release via activation of presynaptic CB1Rs.

4.1. The validity of our data on presynaptic inhibition at PF-PC synapses induced by synthetic cannabinoids

In our experiments, WIN reduced PF-PC EPSC amplitude to 64.5% (1 μM) and 46.8% (10 μM) of the control value using P20–57 mice (Fig. 4*D*). These reductions are comparable to previously published values obtained from acute cerebellar slice preparations: 55.6% of control in 1 μM WIN (P15–21 rats) (Levenes et al., 1998), 29.1 and 12.3% in 1 and 5 μM WIN, respectively (P15–19 rats) (Takahashi and Linden, 2000), and 23.5% in 5 μM WIN (P9–14 mice) (Kawamura et al., 2006). The latter two reports show somewhat smaller percentages compared with our data, but this can be attributed to the differences in the ages of the animals used: an immunohistochemical study revealed that the distribution patterns of CB1Rs in the molecular layer show developmental changes (Kawamura et al., 2006).

Atwood et al. reported that the IC50 of JWH-018 against synaptic transmission is 14.9 nM using autaptic hippocampal neuronal cultures (Atwood et al., 2010), whereas our IC50 value for JWH-018 was approximately 100 times larger than that of their report (Table 1). This discrepancy might be explained by the different neuronal preparations used: Atwood et al. utilized dissociated neuronal cultures, whose synapses would not be wrapped by cell structures such as glial membranes. These synapses would be more easily exposed to CB1R agonists compared with those in cerebellar slice preparations, and therefore synaptic transmission in the autaptic hippocampal cultures might be suppressed by a lower concentration of JWH-018.

Using a binding assay for human recombinant CB1Rs, we recently found that relative IC50s for WIN, MAM-2201, and JWH-018 against CB1Rs were 1.00, 0.70, and 5.30, respectively (Kikura-Hanajiri et al., manuscript in preparation). These data agree well with our observation of the relative IC50s against excitatory neurotransmitter release from PF terminals to PCs using cerebellar slice preparations (Table 1). Therefore, we consider our observations of IC50s in cerebellar preparations to be reasonable.

4.2. Adverse effects of MAM-2201 on targets of the cerebellar cortex and on cerebellum-dependent motor functions

PCs are the sole output GABAergic neurons from the cerebellar cortex and make direct synaptic contacts onto the deep cerebellar nuclear neurons and vestibular nuclear neurons (Voogd and Glickstein, 1998; Zheng and Raman, 2010). PCs receive two types of excitatory input from CFs and PFs. CFs arise from the inferior olivary complex located in the brainstem. CFs are activated during motor learning and induce complex spikes in PCs (Ito, 2001; Llinas et al., 2004). Spikelets in complex spike can propagate to the synaptic terminals of PCs (Khaliq and Raman, 2005). PFs are the axons of granule cells, which are excited by glutamatergic mossy fiber inputs. Mossy fibers originate from nuclei in the spinal cord and brain stem. The mossy fiber-PF pathway is the main operational input to the cerebellum and PCs, and carries afferent information both from the periphery and from other brain centers. PFs produce a brief excitatory postsynaptic potential in PCs that generates a single action potential called a "simple spike." In addition, PCs receive feed-forward synaptic inhibition from GABAergic interneurons, and this inhibition increases the precision of PC spike outputs (Mittmann et al., 2005). Thus, all of these synaptic inputs to PCs can control the output of the cerebellar cortex. The absence of PC activity or genetic manipulation of synaptic transmission from PCs severely affects cerebellum-dependent motor functions: both in mutant mice and in spinocerebellar ataxia type 6 patients, selective degeneration of PCs induce motor dysfunction (Frontali, 2001; Porras-Garcia et al., 2013), and PC-specific vesicular GABA transporter knockout mice exhibit motor impairment (Kayakabe et al., 2013).

We demonstrate that MAM-2201 inhibits neurotransmitter release at PF-PC, interneuron-PC, and CF-PC synapses in a concentration-dependent manner (Figs. 3–6), and reduces the number of spikelets in CF-evoked complex spikes (Fig. 7*A* and *B*). Assuming that, in humans, MAM-2201 inhibits neurotransmitter release at these synapses, the inhibition at PF-PC synapses could cause failure of simple spike generation in PCs. The inhibition of interneuron-PC synapses may weaken the feed-forward inhibition, leading to decreased precision of PC spike outputs. MAM-2201-induced reduction of spikelets in complex spikes (Fig. 7*A* and *B*) could cause a decrease in the number of action potentials that propagate to the synaptic terminals of PCs. Consequently, MAM-2201 may interrupt normal GABAergic inhibition onto the deep cerebellar nuclear neurons and vestibular nuclear neurons, and thus could affect cerebellum-dependent motor coordination. This speculation could be supported by the report that consumption of drugs of abuse containing analogs of MAM-2201 can cause cerebellar dysfunction such as disturbance of finger-to-finger test (Musshoff et al., 2014).

4.3. Possible effects of MAM-2201 on cerebellar LTD initiated by dendritic Ca^{2+} transients and on motor learning functions

PF-PC LTD is thought to underlie cerebellar motor learning in mammals (Yuzaki, 2012). This learning is impaired in transgenic mice that exhibit a deficit in the expression of LTD *in vitro* (Kakegawa et al., 2008). Induction of LTD requires association of PF and CF activation both *in vivo* and *in vitro* (Ito, 2001). At the cellular level, CF synaptic inputs to PCs evoke dendritic Ca^{2+} transients, which play crucial roles in the expression of LTD (Konnerth et al., 1992). Interestingly, Carey and Regehr reported that presynaptic inhibition of CF-PC synapses by noradrenaline alters the complex spike waveform and decreases CF-evoked dendritic Ca^{2+} transients, leading to interference with the induction of LTD (Carey and Regehr, 2009). This noradrenergic modulation shares many features with our observations of MAM-2201-induced changes of CF-evoked responses in PCs (Figs. 6 and 7): depression of CF-PC EPSCs via presynaptic mechanisms, reduction of the number of spikelets in complex spikes, and attenuation of CF-induced Ca^{2+} transients in PC dendrites. Taken together, MAM-2201 may interfere with the induction of LTD *in vitro* and might result in an impairment of cerebellar motor learning *in vivo*. Further work will be needed to clarify whether MAM-2201 indeed blocks the induction of LTD.

4.4. Implications for adverse effects of MAM-2201 on other brain functions

In the brain, CB1Rs are widely and abundantly expressed, and numerous *in vitro* studies have revealed that activation of CB1Rs by agonists suppresses synaptic transmission in several regions such as the hippocampus, nucleus accumbens, striatum, and cerebellar cortex (Kano et al., 2009). Moreover, in rat hippocampal slice preparations, pharmacological activation of CB1Rs modulates long-term potentiation in the CA1 region (Navakkode and Korte, 2014), and *in vivo* administration of WIN impairs hippocampal-dependent short-term memory (Hampson and Deadwyler, 2000). WIN also activates the "reward circuitry" in the brain, including the ventral tegmental area-nucleus accumbens pathway, and alters reward-

related behaviors in a similar manner to other reward-enhancing addictive drugs (Gardner, 2005). In this study, we demonstrated that MAM-2201 suppresses synaptic transmission in the cerebellum and that this action parallels that induced by WIN (Figs. 3–5). Taken together, in humans, MAM-2201 could cause psychoactive effects that are similar to those observed in the laboratory animal experiments using WIN or other synthetic cannabinoids.

Acknowledgments

This work was supported by Health Labour Sciences Research Grants. We thank Dr. Nobutake Hosoi (Gunma University) for technical advice on intracellular Ca^{2+} imaging.

References

Atwood, B.K., Huffman, J., Straiker, A., Mackie, K., 2010. JWH018, a common constituent of 'Spice' herbal blends, is a potent and efficacious cannabinoid CB receptor agonist. Br. J. Pharmacol. 160, 585–593.
Auwarter, V., Dresen, S., Weinmann, W., Muller, M., Putz, M., Ferreiros, N., 2009. 'Spice' and other herbal blends: harmless incense or cannabinoid designer drugs? J. Mass Spectrom. 44, 832–837.
Brown, S.P., Safo, P.K., Regehr, W.G., 2004. Endocannabinoids inhibit transmission at granule cell to Purkinje cell synapses by modulating three types of presynaptic calcium channels. J. Neurosci. 24, 5623–5631.
Bruno, A., Lembo, F., Novellino, E., Stornaiuolo, M., Marinelli, L., 2014. Beyond radiodisplacement techniques for identification of CB1 ligands: the first application of a fluorescence-quenching assay. Sci. Rep. 4, 3757.
Carey, M.R., Regehr, W.G., 2009. Noradrenergic control of associative synaptic plasticity by selective modulation of instructive signals. Neuron 62, 112–122.
Derungs, A., Schwaninger, A.E., Mansella, G., Bingisser, R., Kraemer, T., Liechti, M.E., 2013. Symptoms, toxicities, and analytical results for a patient after smoking herbs containing the novel synthetic cannabinoid MAM-2201. Forensic Toxicol. 31, 164–171.
DeSanty, K.P., Dar, M.S., 2001. Cannabinoid-induced motor incoordination through the cerebellar CB(1) receptor in mice. Pharmacol. Biochem. Behav. 69, 251–259.
Diana, M.A., Levenes, C., Mackie, K., Marty, A., 2002. Short-term retrograde inhibition of GABAergic synaptic currents in rat Purkinje cells is mediated by endogenous cannabinoids. J. Neurosci. 22, 200–208.
Dousmanis, A.G., Pennefather, P.S., 1992. Inwardly rectifying potassium conductances in AtT-20 clonal pituitary cells. Pflugers Arch. 422, 98–104.
Felder, C.C., Joyce, K.E., Briley, E.M., Glass, M., Mackie, K.P., Fahey, K.J., Cullinan, G.J., Hunden, D.C., Johnson, D.W., Chaney, M.O., Koppel, G.A., Brownstein, M., 1998. LY320135, a novel cannabinoid CB1 receptor antagonist, unmasks coupling of the CB1 receptor to stimulation of cAMP accumulation. J. Pharmacol. Exp. Ther. 284, 291–297.
Frontali, M., 2001. Spinocerebellar ataxia type 6: channelopathy or glutamine repeat disorder? Brain Res. Bull. 56, 227–231.
Gardner, E.L., 2005. Endocannabinoid signaling system and brain reward: emphasis on dopamine. Pharmacol. Biochem. Behav. 81, 263–284.
Hagiwara, S., Miyazaki, S., Rosenthal, N.P., 1976. Potassium current and the effect of cesium on this current during anomalous rectification of the egg cell membrane of a starfish. J. Gen. Physiol. 67, 621–638.
Hampson, R.E., Deadwyler, S.A., 2000. Cannabinoids reveal the necessity of hippocampal neural encoding for short-term memory in rats. J. Neurosci. 20, 8932–8942.
Hashimoto, K., Kano, M., 2013. Synapse elimination in the developing cerebellum. Cell. Mol. Life Sci. 70, 4667–4680.
Huestis, M.A., Gorelick, D.A., Heishman, S.J., Preston, K.L., Nelson, R.A., Moolchan, E.T., Frank, R.A., 2001. Blockade of effects of smoked marijuana by the CB1-selective cannabinoid receptor antagonist SR141716. Arch. Gen. Psychiatry 58, 322–328.
Irie, T., Fukui, I., Ohmori, H., 2006. Activation of GIRK channels by muscarinic receptors and group II metabotropic glutamate receptors suppresses Golgi cell activity in the cochlear nucleus of mice. J. Neurophysiol. 96, 2633–2644.
Irie, T., Matsuzaki, Y., Sekino, Y., Hirai, H., 2014. Kv3.3 channels harbouring a mutation of spinocerebellar ataxia type 13 alter excitability and induce cell death in cultured cerebellar Purkinje cells. J. Physiol. 592, 229–247.
Irie, T., Ohmori, H., 2008. Presynaptic GABA(B) receptors modulate synaptic facilitation and depression at distinct synapses in fusiform cells of mouse dorsal cochlear nucleus. Biochem. Biophys. Res. Commun. 367, 503–508.
Ito, M., 2001. Cerebellar long-term depression: characterization, signal transduction, and functional roles. Physiol. Rev. 81, 1143–1195.
Kakegawa, W., Miyazaki, T., Emi, K., Matsuda, K., Kohda, K., Motohashi, J., Mishina, M., Kawahara, S., Watanabe, M., Yuzaki, M., 2008. Differential regulation of synaptic plasticity and cerebellar motor learning by the C-terminal PDZ-binding motif of GluRdelta2. J. Neurosci. 28, 1460–1468.
Kano, M., Ohno-Shosaku, T., Hashimotodani, Y., Uchigashima, M., Watanabe, M., 2009. Endocannabinoid-mediated control of synaptic transmission. Physiol. Rev. 89, 309–380.
Kawamura, Y., Fukaya, M., Maejima, T., Yoshida, T., Miura, E., Watanabe, M., Ohno-Shosaku, T., Kano, M., 2006. The CB1 cannabinoid receptor is the major cannabinoid receptor at excitatory presynaptic sites in the hippocampus and cerebellum. J. Neurosci. 26, 2991–3001.
Kayakabe, M., Kakizaki, T., Kaneko, R., Sasaki, A., Nakazato, Y., Shibasaki, K., Ishizaki, Y., Saito, H., Suzuki, N., Furuya, N., Yanagawa, Y., 2013. Motor dysfunction in cerebellar Purkinje cell-specific vesicular GABA transporter knockout mice. Front. Cell. Neurosci. 7, 286.
Khaliq, Z.M., Raman, I.M., 2005. Axonal propagation of simple and complex spikes in cerebellar Purkinje neurons. J. Neurosci. 25, 454–463.
Kikura-Hanajiri, R., Uchiyama, N., Kawamura, M., Goda, Y., 2013. Changes in the prevalence of new psychoactive substances before and after the introduction of the generic scheduling of synthetic cannabinoids in Japan. Drug Test. Anal..
Konnerth, A., Dreessen, J., Augustine, G.J., 1992. Brief dendritic calcium signals initiate long-lasting synaptic depression in cerebellar Purkinje cells. Proc. Natl. Acad. Sci. U. S. A. 89, 7051–7055.
Korn, H., Faber, D.S., 1991. Quantal analysis and synaptic efficacy in the CNS. Trends Neurosci. 14, 439–445.
Kreitzer, A.C., Regehr, W.G., 2001. Retrograde inhibition of presynaptic calcium influx by endogenous cannabinoids at excitatory synapses onto Purkinje cells. Neuron 29, 717–727.
Kubo, Y., Reuveny, E., Slesinger, P.A., Jan, Y.N., Jan, L.Y., 1993. Primary structure and functional expression of a rat G-protein-coupled muscarinic potassium channel. Nature 364, 802–806.
Kushmerick, C., Price, G.D., Taschenberger, H., Puente, N., Renden, R., Wadiche, J.I., Duvoisin, R.M., Grandes, P., von Gersdorff, H., 2004. Retroinhibition of presynaptic Ca^{2+} currents by endocannabinoids released via postsynaptic mGluR activation at a calyx synapse. J. Neurosci. 24, 5955–5965.
Levenes, C., Daniel, H., Soubrie, P., Crepel, F., 1998. Cannabinoids decrease excitatory synaptic transmission and impair long-term depression in rat cerebellar Purkinje cells. J. Physiol. 510 (Pt 3), 867–879.
Llinas, R., Walton, K.D., Lang, E.J., 2004. Cerebellum. In: Shepard, G.M. (Ed.), The Synaptic Organization of the Brain, fifth ed. Oxford University Press, New York, NY, US, pp. 271–309.
Lonati, D., Buscaglia, E., Papa, P., Valli, A., Coccini, T., Giampreti, A., Petrolini, V.M., Vecchio, S., Serpelloni, G., Locatelli, C.A., 2014. MAM-2201 (analytically confirmed) intoxication after "synthacaine" consumption. Ann. Emerg. Med..
Luk, T., Jin, W., Zvonok, A., Lu, D., Lin, X.Z., Chavkin, C., Makriyannis, A., Mackie, K., 2004. Identification of a potent and highly efficacious, yet slowly desensitizing CB1 cannabinoid receptor agonist. Br. J. Pharmacol. 142, 495–500.
Mackie, K., 2008. Signaling via CNS cannabinoid receptors. Mol. Cell. Endocrinol. 286, S60–S65.
Mackie, K., Lai, Y., Westenbroek, R., Mitchell, R., 1995. Cannabinoids activate an inwardly rectifying potassium conductance and inhibit Q-type calcium currents in AtT20 cells transfected with rat brain cannabinoid receptor. J. Neurosci. 15, 6552–6561.
Maejima, T., Hashimoto, K., Yoshida, T., Aiba, A., Kano, M., 2001. Presynaptic inhibition caused by retrograde signal from metabotropic glutamate to cannabinoid receptors. Neuron 31, 463–475.
McKay, B.E., Turner, R.W., 2005. Physiological and morphological development of the rat cerebellar Purkinje cell. J. Physiol. 567, 829–850.
Mittmann, W., Koch, U., Hausser, M., 2005. Feed-forward inhibition shapes the spike output of cerebellar Purkinje cells. J. Physiol. 563, 369–378.
Monory, K., Blaudzun, H., Massa, F., Kaiser, N., Lemberger, T., Schutz, G., Wotjak, C.T., Lutz, B., Marsicano, G., 2007. Genetic dissection of behavioural and autonomic effects of Delta(9)-tetrahydrocannabinol in mice. PLoS Biol. 5, e269.
Moosmann, B., Kneisel, S., Girreser, U., Brecht, V., Westphal, F., Auwarter, V., 2012. Separation and structural characterization of the synthetic cannabinoids JWH-412 and 1-[(5-fluoropentyl)-1H-indol-3yl]-(4-methylnaphthalen-1-yl)methanone using GC-MS, NMR analysis and a flash chromatography system. Forensic Sci. Int. 220, e17–22.
Musshoff, F., Madea, B., Kernbach-Wighton, G., Bicker, W., Kneisel, S., Hutter, M., Auwarter, V., 2014. Driving under the influence of synthetic cannabinoids ("Spice"): a case series. Int. J. Legal Med. 128, 59–64.
Navakkode, S., Korte, M., 2014. Pharmacological activation of CB1 receptor modulates long term potentiation by interfering with protein synthesis. Neuropharmacology 79, 525–533.
Patel, S., Hillard, C.J., 2001. Cannabinoid CB(1) receptor agonists produce cerebellar dysfunction in mice. J. Pharmacol. Exp. Ther. 297, 629–637.
Porras-Garcia, M.E., Ruiz, R., Perez-Villegas, E.M., Armengol, J.A., 2013. Motor learning of mice lacking cerebellar Purkinje cells. Front. Neuroanat. 7, 4.
Regehr, W.G., Carey, M.R., Best, A.R., 2009. Activity-dependent regulation of synapses by retrograde messengers. Neuron 63, 154–170.
Safo, P.K., Cravatt, B.F., Regehr, W.G., 2006. Retrograde endocannabinoid signaling in the cerebellar cortex. Cerebellum 5, 134–145.
Safo, P.K., Regehr, W.G., 2005. Endocannabinoids control the induction of cerebellar LTD. Neuron 48, 647–659.
Saito, T., Namera, A., Miura, N., Ohta, S., Miyazaki, S., Osawa, M., Inokuchi, S., 2013. A fatal case of MAM-2201 poisoning. Forensic Toxicol. 31, 333–337.
Seely, K.A., Lapoint, J., Moran, J.H., Fattore, L., 2012. Spice drugs are more than harmless herbal blends: a review of the pharmacology and toxicology of synthetic cannabinoids. Prog. Neuro Psychopharmacol. Biol. Psychiatry 39, 234–243.

Shen, M., Thayer, S.A., 1999. Delta9-tetrahydrocannabinol acts as a partial agonist to modulate glutamatergic synaptic transmission between rat hippocampal neurons in culture. Mol. Pharmacol. 55, 8–13.
Showalter, V.M., Compton, D.R., Martin, B.R., Abood, M.E., 1996. Evaluation of binding in a transfected cell line expressing a peripheral cannabinoid receptor (CB2): identification of cannabinoid receptor subtype selective ligands. J. Pharmacol. Exp. Ther. 278, 989–999.
Shuvaev, A.N., Horiuchi, H., Seki, T., Goenawan, H., Irie, T., Iizuka, A., Sakai, N., Hirai, H., 2011. Mutant PKC{gamma} in spinocerebellar ataxia type 14 disrupts synapse elimination and long-term depression in Purkinje cells in vivo. J. Neurosci. 31, 14324–14334.
Szabo, B., Than, M., Thorn, D., Wallmichrath, I., 2004. Analysis of the effects of cannabinoids on synaptic transmission between basket and Purkinje cells in the cerebellar cortex of the rat. J. Pharmacol. Exp. Ther. 310, 915–925.
Takahashi, K.A., Linden, D.J., 2000. Cannabinoid receptor modulation of synapses received by cerebellar Purkinje cells. J. Neurophysiol. 83, 1167–1180.
Taura, F., Sirikantaramas, S., Shoyama, Y., Shoyama, Y., Morimoto, S., 2007. Phytocannabinoids in Cannabis sativa: recent studies on biosynthetic enzymes. Chem. Biodivers. 4, 1649–1663.
Uchiyama, N., Kawamura, M., Kikura-Hanajiri, R., Goda, Y., 2013. URB-754: a new class of designer drug and 12 synthetic cannabinoids detected in illegal products. Forensic Sci. Int. 227, 21–32.
Vardakou, I., Pistos, C., Spiliopoulou, C., 2010. Spice drugs as a new trend: mode of action, identification and legislation. Toxicol. Lett. 197, 157–162.
Vincent, P., Marty, A., 1996. Fluctuations of inhibitory postsynaptic currents in Purkinje cells from rat cerebellar slices. J. Physiol. 494 (Pt 1), 183–199.
Voogd, J., Glickstein, M., 1998. The anatomy of the cerebellum. Trends Cogn. Sci. 2, 307–313.
Wilson, R.I., Nicoll, R.A., 2002. Endocannabinoid signaling in the brain. Science 296, 678–682.
Xu-Friedman, M.A., Regehr, W.G., 1999. Presynaptic strontium dynamics and synaptic transmission. Biophys. J. 76, 2029–2042.
Yuzaki, M., 2012. Cerebellar LTD vs. motor learning-lessons learned from studying GluD2. Neural Netw..
Zheng, N., Raman, I.M., 2010. Synaptic inhibition, excitation, and plasticity in neurons of the cerebellar nuclei. Cerebellum 9, 56–66.
Zucker, R.S., Regehr, W.G., 2002. Short-term synaptic plasticity. Annu Rev. Physiol. 64, 355–405.

The Journal of Toxicological Sciences (J. Toxicol. Sci.)
Vol.38, No.3, ***-***, 2013

Toxicomics Report

Comparative gene expression analysis of the amygdala in autistic rat models produced by pre- and post-natal exposures to valproic acid

Atsuko Oguchi-Katayama[1], Akihiko Monma[2], Yuko Sekino[1], Toru Moriguchi[2] and Kaoru Sato[1]

[1]Laboratory of Neuropharmacology, Division of Pharmacology, National Institute of Health Sciences, 1-18-1 Kamiyoga, Setagaya-ku, Tokyo 158-8501, Japan
[2]Department of Food and Life Sciences, Azabu University, 1-17-71 Fuchinobe, Tyuoku, Sagamihara-shi, Kanagawa 252-5201, Japan

(Received October 24, 2012; Accepted March 14, 2013)

ABSTRACT — Gene expression profiles in the amygdala of juvenile rats were compared between the two autistic rat models for mechanistic insights into impaired social behavior and enhanced anxiety in autism. The rats exposed to VPA by intraperitoneal administration to their dams at embryonic day (E) 12 were used as a model for autism (E2IP), and those by subcutaneous administration at postnatal day (P) 14 (P14SC) were used as a model for regressive autism; both of the models show impaired social behavior and enhanced anxiety as symptoms. Gene expression profiles in the amygdala of the rats (E12IP and P14SC) were analyzed by microarray and compared to each other. Only two genes, Neu2 and Mt2a, showed significant changes in the same direction in both of the rat models, and there were little similarities in the overall gene expression profiles between them. It was considered that gene expression changes per se in the amygdala might be an important cause for impaired social behavior and enhanced anxiety, rather than expression changes of particular genes.

Key words: Valproic acid, Amygdala, Microarray, Prenatal, Postnatal

INTRODUCTION

There are two similar but different kinds of autistic animal models produced by perinatal exposure of rodents to valproic acid (VPA). Rodents exposed to VPA on embryonic day (E) 12 have been used as an animal model for autism characterized by impaired social behavior, enhanced anxiety, and decreased sensitivity to pain after maturation (Markram *et al.*, 2008; Schneider and Przewtocki, 2005; Schneider *et al.*, 2007, 2008). On the other hand, rodents exposed to VPA on postnatal day (P) 14 have been used as an animal model for regressive autism that shows impaired social behavior like animal models for autism but accompanied by loss of some acquired skills (Yochum *et al.*, 2008, 2010; Wagner *et al.*, 2006). The regressive autism model also showed enhanced anxiety in our preliminary study.

The amygdala has been considered critical for behaviors associated with emotional disorders. Possible mechanisms of impaired social behavior in autism involve neural networks including the amygdala (Neuhaus *et al.*, 2010). The amygdala has also been identified to be involved in anxiety behaviors (Blackford and Pine, 2012). In humans, the amygdala and prefrontal cortex is the responsible for anxiety disorders (Etkin and Wager, 2007). It is therefore expected that comparative analysis of the amygdala in the two animal models for autism provide some mechanistic insights into impaired social behavior and enhanced anxiety in autism from similarities between them.

In the present study, we performed comparative gene expression analysis of the amygdala and characterize the similarities between the animal models for autism and for regressive autism. We first confirmed the effect of postnatal exposure to VPA on anxiety-related behavior in rats. We then compared gene expression profiles in the amygdala of juvenile rats between prenatal and postnatal exposures to VPA.

Correspondence: Kaoru Sato (E-mail: kasato@nihs.go.jp)

MATERIALS AND METHODS

Animals and VPA treatment

Pregnant Wistar Hannover/Rcc rats were obtained from Japan SLC, Inc. (Shizuoka, Japan) and maintained individually under conventional conditions with controlled temperature (23 ± 3°C) and illumination (12 hr; 7:00-19:00). Each of five litters was culled to 10 pups/litter on day 2 after birth for matched nursing conditions. For postnatal exposure, saline or 400 mg/kg of VPA (Sigma, St. Louis, MO, USA) was administered subcutaneously (s.c.) to half of the pups in each litter on postnatal day 14 (P14SC). For prenatal exposure, saline or 600 mg/kg of VPA was administered intraperitoneally (i.p.) to five pregnant rats on E12 (E12IP). Microarray analysis was performed at 5 (E12IP and P14SC) or 7 (P14SC7w) wks after the VPA administrations (Fig. 1). All animal treatments and experimental protocols were approved by the Animal Care and Use Committee of the Azabu University and the National Institute of Health Science (NIHS), and followed the Guide for the Care and Use of Laboratory Animals.

Behavioral test for anxiety

As a behavioral test, elevated plus maze (EPM) was performed in P14SC at 5 wks old with a maze consists of two opposite open arms (50 × 10 cm) and two opposite enclosed arms. The arms are connected by a central 10-cm square, forming a plus shape. The maze was elevated 50 cm above the floor. The animal's path was observed for 5 min after a resting period of 2 min in the central square of the maze. The number of entries into the open arms and the time spent in the open arms were measured.

Microarray analysis

Microarray analysis was performed using animals different from those used for behavioral test. The amygdalae were removed from the juvenile rats, and incubated in a RNA stabilization solution (RNAlater, Ambion, Austin, TX, USA) (1 ml for 5 x 5 x 5 (mm) block) overnight. Total RNA samples from the amygdalae were isolated with TRIzol (Invitrogen, Carlsbad, CA, USA) and the RNeasy Mini Kit (Qiagen, Hilden, Germany), with slight modifications to the manufacturer's protocol. The

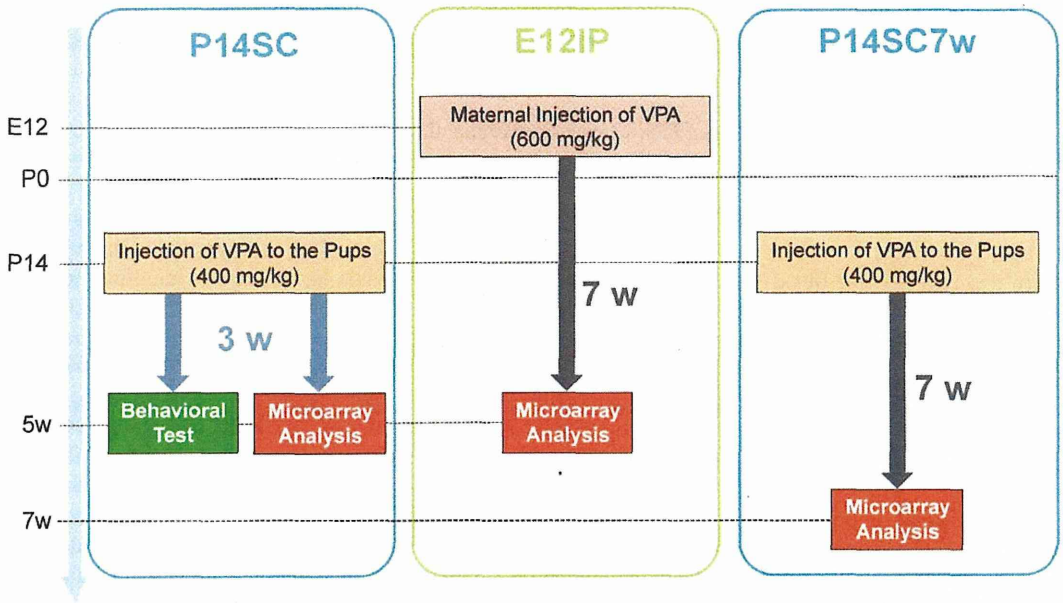

Fig. 1. The experimental design. To investigate the effect of postnatal VPA exposure on behavior and gene expression profiles, saline or 400 mg/kg VPA was administered to half of the pups per one litter subcutaneously on postnatal day 14 (P14SC). Behavior test and microarray analysis were performed using individual animals. To avoid influence of the dams, 5w juvenile rats (P35-37) were obtained evenly from 5 litters for control group and VPA- treated group, respectively. To investigate the effect of prenatal exposure, five pregnant rats were treated intraperitoneally (i.p.) with saline or 600 mg/kg VPA on E12.5 (E12IP), respectively, and microarray analysis was performed at 5w (P35-37). To analyze the contribution of the length of time from VPA exposure to cRNA isolation to the change in gene expression profile, microarray analysis was also performed at 7w (P49-56) (5 w after VPA exposure at P14) (P14SC7w).

isolated RNA sample (100 μg) were used for the microarray analysis (Affymetrix GeneChip Rat Genome 230 2.0 array (Santa Clara, CA, USA)) according to the Affymetrix protocol (http://www.affymetrix.com/support/technical/manuals.affx). Data were collected using Affymetrix GeneChip® Operating Software (GCOS) (http://media.affymetrix.com/support/technical/whitepapers/sadd_whitepaper.pdf).

Data analysis

Data analyses were carried out with GeneSpring (Agilent Technologies, Santa Clara, CA, USA). All of the data from the VPA-treated groups were normalized to the median of the control groups, and the expression of each selected gene was calculated as a log ratio of the signal to the control value. To assess the differences between the control and VPA-treated groups, the Benjamini and Hochberg false-discovery rate (FDR) method was employed, and those with a p-value less than 0.05 were considered as significant. Network, function, and pathway analyses were performed using Ingenuity Pathway Analysis software (IPA; Ingenuity Systems, Redwood City, CA, USA).

RESULTS AND DISCUSSION

Behavioral tests for anxiety

The time spent in the open arms was significantly shorter in the males of P14SC than in those of the corresponding control, indicating enhanced anxiety by postnatal exposure to VPA (Fig. 2, left). There were, however, no significant changes in the behavior test of the females (Fig. 2, right). There were no effects of the VPA exposure on the number of entries into the open arms in both genders (data not shown). These results indicate that postnatal exposure to VPA caused enhanced anxiety specifically in males. This sexual dimorphism is a typical feature of autism and has been observed in the animal model for autism produced by prenatal exposure to VPA (Schneider *et al.*, 2008). We therefore analyzed the gene expression profile of the amygdala exposed to VPA only in males in the following experiments.

Gene expression microarray analysis

In the controls, gene expression profiles were almost identical among the varied VPA exposure conditions. The number of genes with expression levels different from those in the corresponding controls was larger in P14SC (53 probe sets for 49 genes) than in E12IP (32 probe sets for 30 genes), excluding expressed sequence tags (Fig. 3A). Functional classification of the genes also indicated the differences of gene expression between P12IP and P14SC (Fig. 3B). P14SC contained a wider variety of categories than E12IP; 'phosphatase' appeared only in E12IP, while 'cytokine', 'growth factor', 'lig-

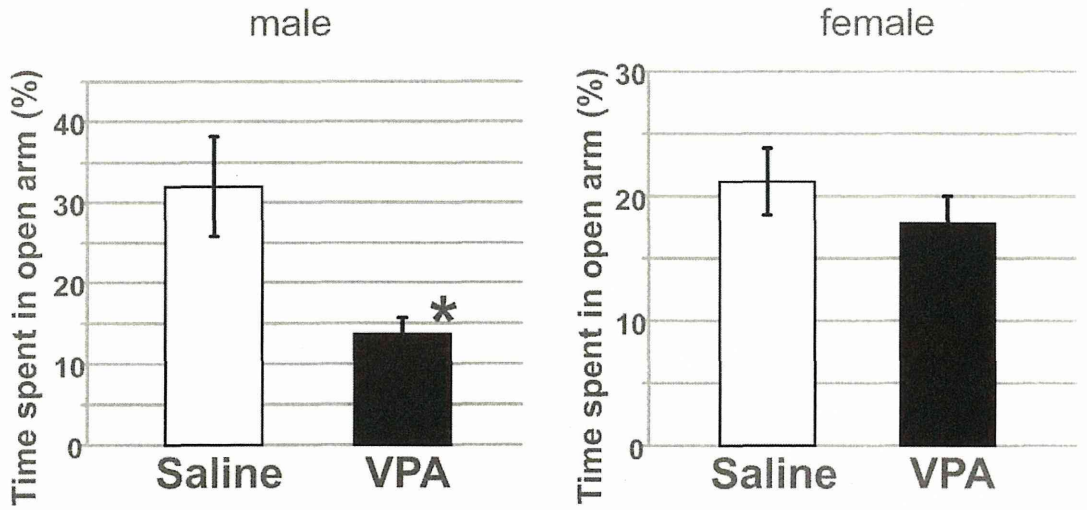

Fig. 2. The effects of postnatal exposure to VPA on anxiety-related behavior. 400 mg/kg VPA was administered to animals subcutaneously at P14. Anxiety-related behaviors were analyzed at 5w by EPM. Total open arm entries and time spent in open arm are quantified. The data of time spent in open arm were shown. An asterisk indicates a statistically significant difference from the control ($P < 0.05$, $N = 13$-15, Student's t test).

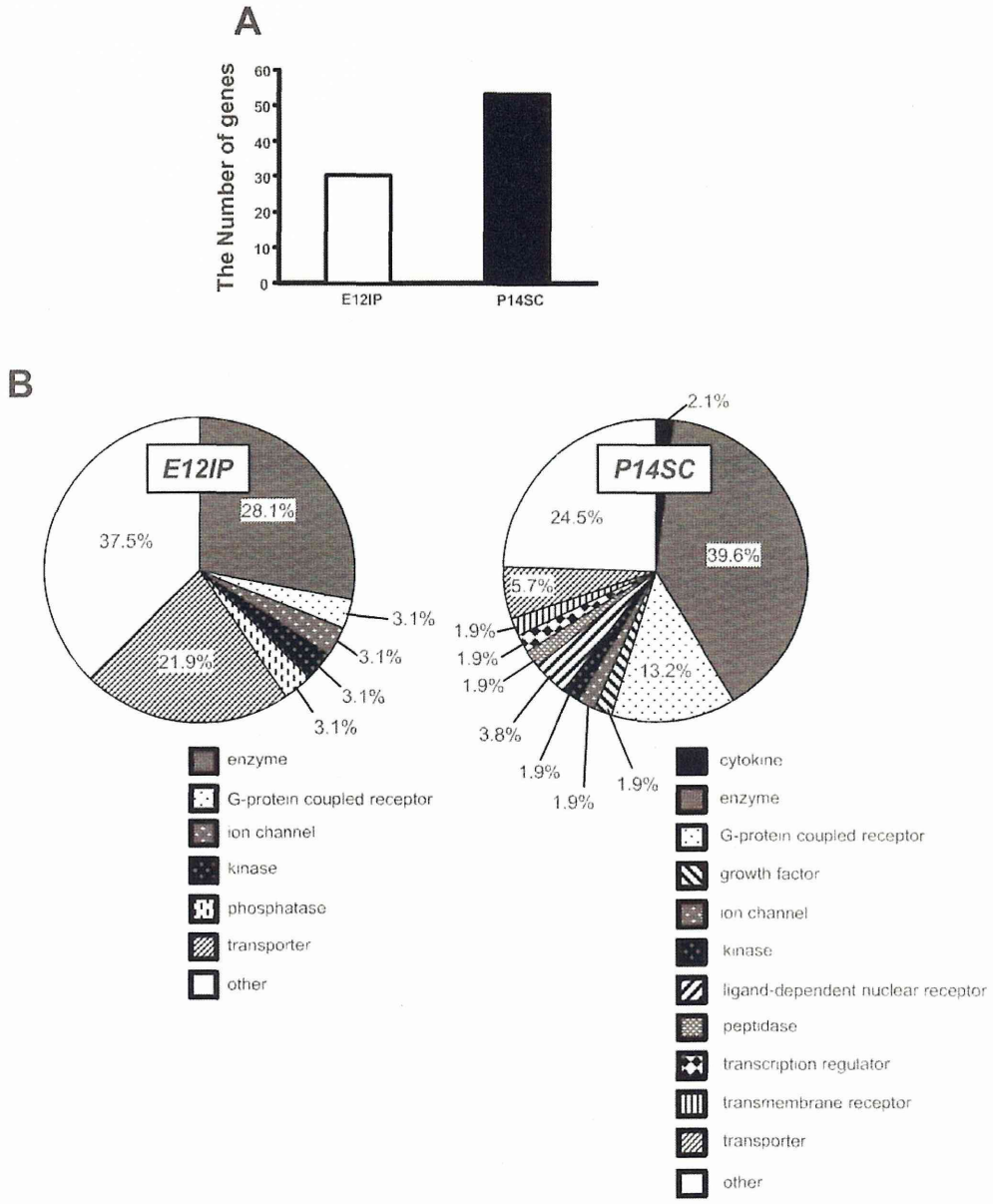

Fig. 3. Summary of the gene expression profiles of E12IP and P14SC rats (male). For both of E12IP and P14SC, total RNA of the amygdalae of 5w male rats (P33-37, N = 4) were analyzed with the microarray chip. Data were collected using Affymetrix GeneChip® Operating Software (GCOS) and analyzed using GeneSpring software. A. The numbers of significantly changed genes in E12IP and P14SC ($p < 0.05$, N = 4). B. Functional classification of the significantly changed genes by GeneSpring.

and-dependent nuclear receptor', 'peptidase', 'transcription regulator', and 'transmembrane receptor' appeared only in P14SC. As for categories common to E12IP and P14SC, their proportions were different from each other; e.g., 'transporters' accounted for 21.9% in E12IP but only 5.7% in P14SC.

Only two genes, Neu2 and Mt2a, exhibited the significant changes in the same direction in E12IP and P14SC

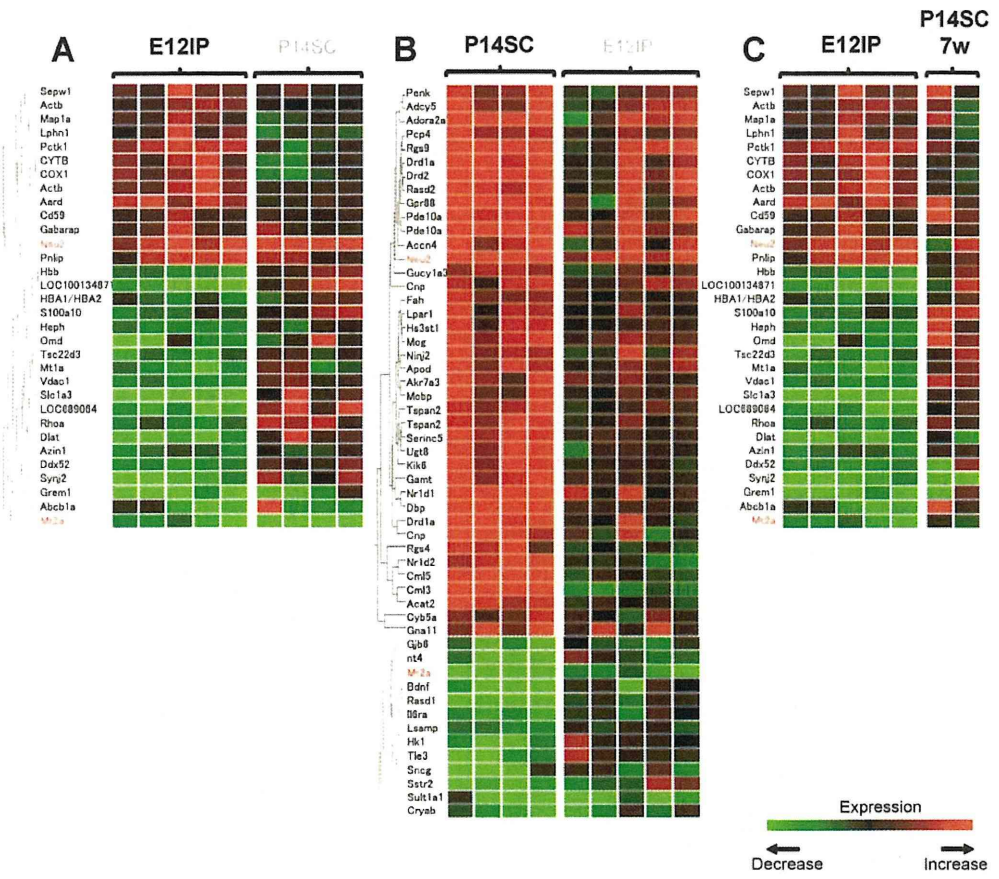

Fig. 4. Heat maps representing hierarchical clustering of the significantly changed genes of E12IP and P14SC. Each vertical column represents an individual sample, and each horizontal row represents a single gene. (N = 4 for P14SC and E12IP, N = 2 for P14SC7w) A. A heat map/hierarchical clustering of the significantly changed genes of E12IP with a heat map of the same genes of P14SC. Clustering was performed using the Benjamini and Hochberg FDR method. B. A heat map/hierarchical clustering of the significantly changed genes of P14SC with a heat map of the same genes of E12IP. C. A heat map of E12IP was compared with that of P14SC7w in which cRNA was extracted 7 w after VPA exposure at P14.

(red letters in Figs. 4A and B). The expression profile in E12IP was also different from that in P14SC7w (Fig. 4C), suggesting that the differences between E12IP and P14SC were not due to the varied length of time between the VPA exposure and the gene expression analysis. Precise gene lists for the heat maps of E12IP (Fig. 4A) and P14SC (Fig. 4B) are shown in Table 1 and Table 2, respectively. 'Behavior'-related genes were identified only in P14SC (Table 3). A larger number of genes were categorized as 'nervous system development and function', 'neurological disease' and 'psychological disorders' in P14SC than in E12IP.

Pathway analysis

The most significantly changed network (Fig. 5A [i]) was that linking 'cell death', 'cellular compromise', and 'neurological disease'. The hubs of this network were MYC, HTT, and CASP3, although the expression levels of these three genes remained unchanged. The second most significantly changed network was that linking 'cell death', 'neurological disease', and 'carbohydrate metabolism' (Fig. 5A [ii]). TNF, which plays an especially important role in cell death, was a highly interconnected node. In P14SC, three significant networks were identified (Fig. 5B [i]-[iii]). These networks are related to 'nucleic acid metabolism' (Fig. 5B [i]), 'cell signaling' (Fig. 5B

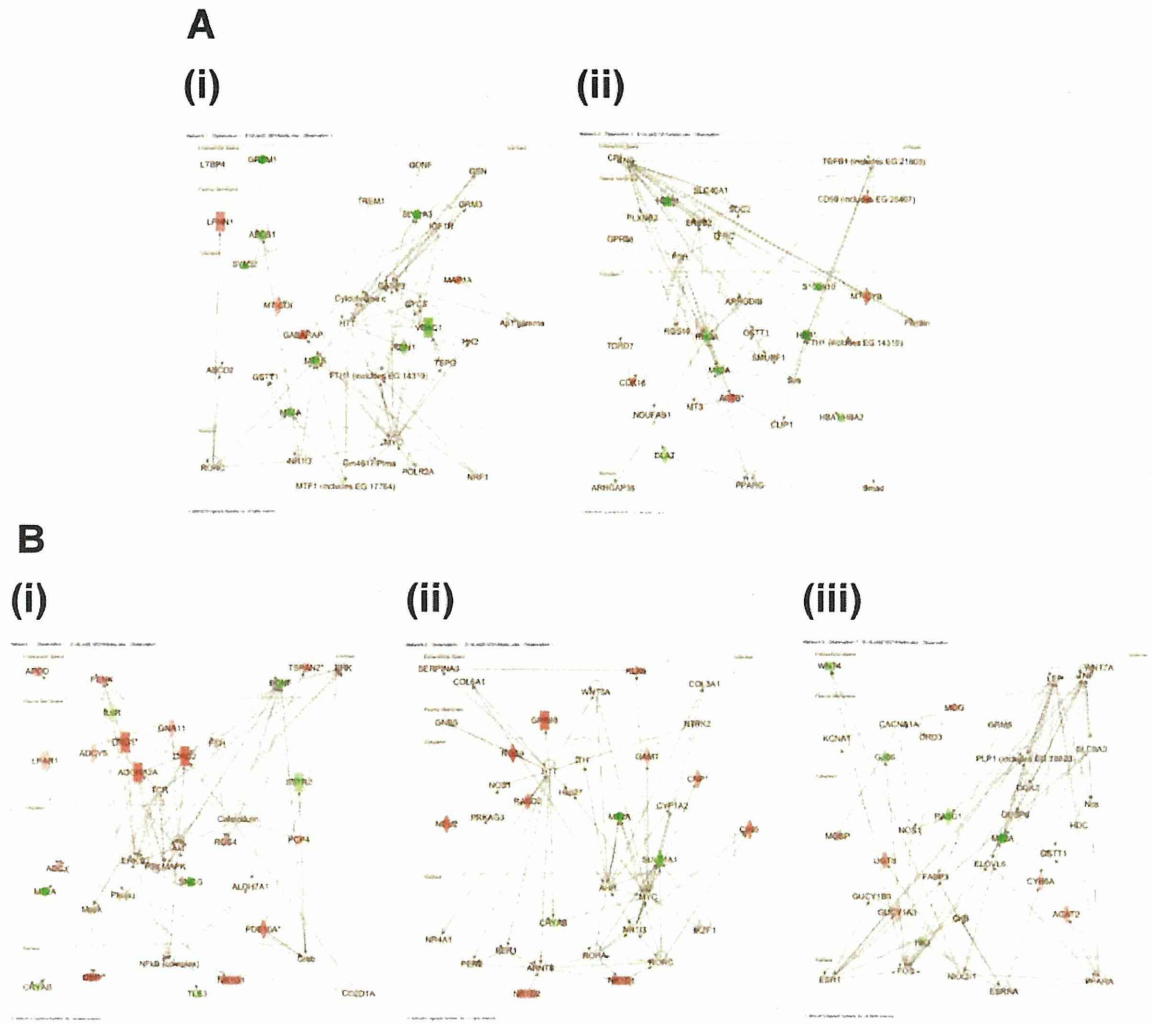

Fig. 5. IPA networks generated with significantly changed genes of E12IP and P14SC. A. The first (i) and second (ii) most significantly altered networks in E12IP. The most significantly changed network linked 'cell death', 'cellular compromise', and 'neurological disease'. The second most significantly changed network linked 'cell death', 'neurological disease', and 'carbohydrate metabolism'. B. The first (i), second (ii), and third (iii) most significantly changed networks in P14SC. These networks are related to 'nucleic acid metabolism' (i), 'cell signaling' (ii), and 'neurological disease' (iii).

[ii]), and 'neurological disease' (Fig. 5B [iii]). One notable aspect of these networks that was not observed in the E12IP networks is the alterations in the expression levels of nuclear genes such as DBP (transcription regulator), NR1D1 (nuclear receptor), and NR1D2 (nuclear receptor).

In conclusion, there are little similarities in the gene expression profiles between the two rat models for autism and regressive autism produced by pre- and post-natal exposures to VPA respectively. It is considered that that gene expression changes per se in the amygdala may be an important cause for impaired social behavior and enhanced anxiety, rather than expression changes of particular genes.

Table 1. The list of genes which changed significantly in E12IP

ID	Symbol	Entrez Gene name	Type(s)
Increase			
1389956_a_at	MT-COI	cytochrome c oxidase subunit I	enzyme
1367996_a_at	LPHN1	latrophilin 1	G-protein coupled receptor
1367882_at	MAP1A	microtubule-associated protein 1A	other
1388159_at	MT-CYB	cytochrome b	enzyme
1367929_at	CD59 (includes EG:25407)	CD59 molecule, complement regulatory protein	other
1398836_s_at	ACTB	actin, beta	other
1368127_at	NEU2	sialidase 2 (cytosolic sialidase)	enzyme
1398835_at	ACTB	actin, beta	other
1370326_at	CDK16	cyclin-dependent kinase 16	kinase
1370804_at	GABARAP	GABA(A) receptor-associated protein	transporter
1367593_at	SEPW1	selenoprotein W, 1	enzyme
1368554_at	PNLIP	pancreatic lipase	enzyme
1370459_at	C8orf85	chromosome 8 open reading frame 85	other
Decrease			
1387197_at	OMD	osteomodulin	other
1371245_a_at	HBB	hemoglobin, beta	transporter
1371130_at	SLC1A3	solute carrier family 1 (glial high affinity glutamate transporter), member 3	transporter
1368971_a_at	SYNJ2	synaptojanin 2	phosphatase
1371102_x_at	LOC100134871	beta globin minor gene	other
1369113_at	GREM1	gremlin 1	other
1371237_a_at	MT1E	metallothionein 1E	other
1368533_at	HEPH	hephaestin	transporter
1368588_at	DDX52	DEAD (Asp-Glu-Ala-Asp) box polypeptide 52	enzyme
1367771_at	Tsc22d3	TSC22 domain family, member 3	other
1386909_a_at	VDAC1	voltage-dependent anion channel 1	ion channel
1388271_at	MT2A	metallothionein 2A	other
1370464_at	ABCB1	ATP-binding cassette, sub-family B (MDR/TAP), member 1	transporter
1367553_x_at	HBB	hemoglobin, beta	transporter
1386890_at	S100A10	S100 calcium binding protein A10	other
1370575_a_at	AZIN1	antizyme inhibitor 1	enzyme
1370130_at	RHOA	ras homolog gene family, member A	enzyme
1388194_at	DLAT	dihydrolipoamide S-acetyltransferase	enzyme
1388608_x_at	HBA1/HBA2	hemoglobin, alpha 1	transporter

ID, symbol, entrez gene name, type of each gene were shown based on IPA software database.